SCIENCE CHINA
Technological Sciences

December 2011 Vol.54 Suppl. 1: 167–174
doi: 10.1007/s11431-011-4637-0

In situ experiments on width and evolution characteristics of excavation damaged zone in deeply buried tunnels

LI ShaoJun[1*], FENG XiaTing[1], LI ZhanHai[3], CHEN BingRui[1], JIANG Quan[1], WU ShiYong[2], HU Bin[2] & XU JinSong[2]

[1] *State Key Laboratory of Geomechanics and Geotechinical Engineering, Institute of Rock and Soil Mechanics, Chinese Academy of Sciences, Wuhan 430071, China;*
[2] *Ertan Hydropower Development Company, Ltd., Chengdu 610051, China;*
[3] *School of Resources and Civil Engineering, Northeastern University, Shenyang 110004, China*

Received July 9, 2011; accepted September 12, 2011; published online November 18, 2011

The seven long tunnels of Jinping II hydropower station are deeply buried. The width and evolution characteristics of excavation damaged zone (EDZ) are the key problem to the design of tunnels excavation and supports. In order to study this problem, several specific experimental tunnels with different overburden and geometric sizes were excavated at this site. Digital borehole camera, sliding micrometer, cross-hole acoustic wave equipment and acoustic emission apparatus were adopted. This paper introduced the comprehensive *in situ* experimental methods through pre-installed facilities and pre-drilled boreholes. Typical properties of the surrounding rock mass, including cracks, deformation, elastic wave and micro fractures, were measured during the whole process of the tunnel excavation. The width and characteristics of formation and evolution of tunnels EDZ were analyzed under different construction methods involving of TBM and drilling and blasting, the test tunnels were excavated by full-face or two benches. The relationships between EDZ and tunnel geometry sizes, overburden and excavation method were described as well. The results will not only contribute a great deal to the analysis of rock mass behavior in deeply buried rock mass, but also provide direct data for support design and rockburst prediction.

deeply buried tunnel, excavation damaged zone, evolution characteristics, *in situ* experiments

Citation: Li S J, Feng X T, Li Z H, et al. *In situ* experiments on width and evolution characteristics of excavation damaged zone in deeply buried tunnels. Sci China Tech Sci, 2011, 54(Suppl. 1): 167–174, doi: 10.1007/s11431-011-4637-0

1 Introduction

In recent years, underground projects and laboratories for hydroelectricity, mining, physics, biology and geoscience have been very popular. The excavation damaged zone (EDZ) under high levels of geo-stress is a key problem to the stability of underground rock engineering. The width, formation and evolution of the EDZ are still difficult problems to solve. Fortunately, many studies on theoretical analysis and mechanical modelling in this subject have been implemented [1–5]. However, there is still little research done related to deeply buried tunnels or caverns. Some deep underground rock engineering projects in the world [6–12] are listed in Table 1, it can be seen that the tunnels in Jinping II hydropower station have almost the maximum overburden for the study of rock mechanics and physics.

In situ tests providing direct data are always the key content for the study of rock mechanics and engineering. The normal methods of EDZ field tests include acoustic waves [6–9, 11, 12], acoustic emissions [9, 13], rock permeability [11, 14] and displacement by extensometer and sliding mi-

*Corresponding author (email: sjli@whrsm.ac.cn)

crometer [11]. Previous researches on field tests were mainly to obtain the width of EDZ. As we know, due to the complex and variable geological settings and different construction conditions of rock engineering, the characteristics of EDZ are often different. In addition, there are few researches on EDZ formation and evolution during the construction process of deeply buried projects.

In order to investigate the width and evolution characteristics of EDZ, several underground experimental tunnels with different overburden and geometric sizes have been excavated at the site of Jinping II hydropower station, China. This paper introduces the comprehensive testing methods such as the digital borehole camera, sliding micrometer and cross-hole acoustic wave and acoustic emission techniques. Based on the testing data of cracks, deformation, elastic wave and micro fractures of surrounding rock mass, the width, formation and evolution process of EDZ are given under different construction conditions such as TBM and drilling and blasting. The test tunnels were excavated by full-face or two benches. In addition, the relationships between EDZ and tunnel geometry sizes, overburden and excavation method are also discussed.

2 Site description and configuration

The Jinping II hydroelectric power station is located on the Great Jinping River Bend of the Yalong River, Sichuan Province, China. It is one of the most outstanding tunnelling projects in the world and has some of the world's longest and deepest hydroelectric tunnels [15]. The power station utilizes a 310 m natural head from the Jinping I scheme for power generation. There are seven parallel high pressure tunnels with the maximum overburden of 2525 m. Two of the tunnels used for transportation are named auxiliary tunnels *A* and *B*, the other one is for drainage, and the rest four, are headrace tunnels with an average length of 16.7 km. The tunnels are being excavated for marble, sandstone and slate. A series of large faults and folds are distributed along them.

Table 1 Some major projects of deep underground rock engineering

Project name	Country	Rock type	Maximum overburden (m)
KAERI	Korea	Crystalline	500
AECL	Canada	Granite	420
ASPO	Sweden	Granite	450
GRIMSEL	Switzerland	Granite	450
TONO	Japan	Granite	1000
SOUDAN	USA	Volcanic tuff	850
Jinping II	China	Marble	2525

The experimental tunnels can be divided into three zones named JPTSA-2, JPTSA-3 and JPTY-21, respectively. The former two lie to the south of auxiliary tunnel *A* and the latter is located at the north of the No.3 headrace tunnel. The configuration of the tunnels is shown in Figure 1 and the relevant properties are listed in Table 2. It can be seen that the tunnels are in different sectional shapes, geometry sizes, burial depths, excavation methods and lithology.

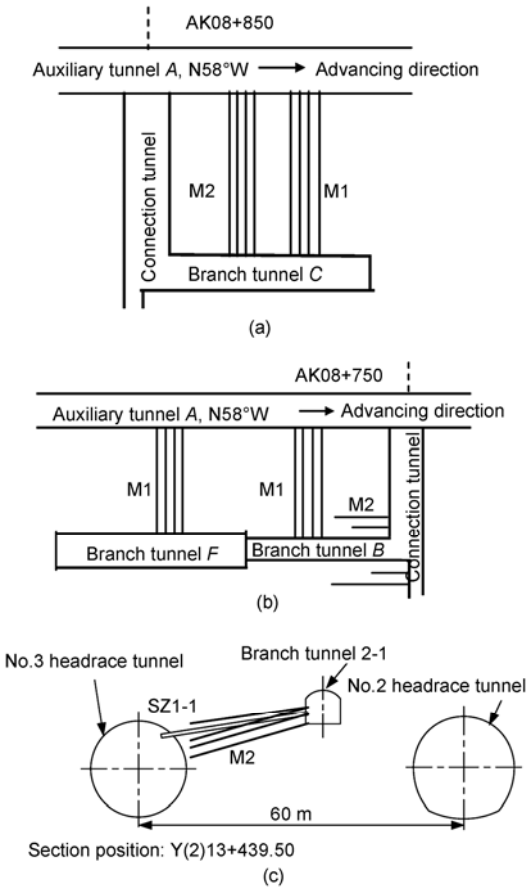

Figure 1 Configuration of experimental tunnels. (a) Experimental zone of JPTSA-2; (b) experimental zone of JPTSA-3; (c) experimental zone of JPTY-21.

Table 2 Some properties of experimental tunnels

Tunnel No.	Section shape	Geometry size (m)	Length of tunnel (m)	Burial depth (m)	Excavation method	Lithology
Branch *B*	arch	5.0×5.0	30	2370	D&B [a], Full face	marble (T_{2b})
Branch *C*	arch	3.0×2.2	30	2430	D&B, Full face	
Branch *F*	arch	7.5×8.0	40	2370	D&B, different bench	
Branch 2-1	arch	5.0×5.0	25	1900	D&B, Full face	marble (T_2y^5)
Auxiliary *A*	arch	6.7×6.3	17500	0–2375	D&B, Full face	marble, sandstone and slate
No.2 headrace tunnel	horseshoe	ϕ13.0	16660	0–2525	D&B, Full face	
No.3 headrace tunnel	circle	ϕ12.4	16670	0–2525	TBM, Full face	

a) Drilling and blasting method

Figure 2 Construction site of experimental branch tunnels *B* and *F*.

The test tunnels for EDZ testing in different experimental zones are branch tunnels *C*, *B*, and *F* and No.3 headrace tunnel. Figure 2 shows the picture of construction site of branch tunnels *B* and *F*.

3 Experimental methods and facilities

According to the configuration of the experimental tunnels described above, in order to obtain the EDZ of testing tunnels to be excavated, the monitoring facilities are pre-installed and testing boreholes pre-drilled in the surrounding rock mass through the excavated tunnels. Elastic waves, cracks, deformation and micro fractures are to be measured during the whole process of tunnels excavation. The corresponding facilities include cross-hole acoustic wave equipment, digital borehole camera, sliding micrometer and acoustic emissions apparatus.

3.1 Definition of EDZ

At present, the EDZ has different concepts and is often defined according to the project type, testing methods and research goals. There are three main conceptions on the EDZ definition. Firstly. the EDZ is the region where the acoustic wave decreases significantly [2, 6, 9, 10]; Secondly, the EDZ is regarded as the region where the rock properties and conditions have changed due to fracturing, stress redistribution and desaturation [10]; Thirdly, the EDZ is defined by measurable and permanent changes to the mechanical and hydraulic transport properties of the rock surrounding the excavation [7]. On the other hand, the division of EDZ is also different. KWON S divided the EDZ into zone I and zone II based on the variable acoustic wave of the rock mass [6]. T. Sato considered that the EDZ consisted of the excavation damaged zone, stress redistributed zone and unsaturated zone [9]. Martino regards the EDZ as the inner and outer damage zones [7, 12].

In this paper, according to the project demands and measurable conditions, the excavation damaged zone is defined the rock zone around tunnel with permanent changes to the mechanical and hydraulic transport properties. It is divided into macro-fracturing zone (EDZ) and outer disturbed zone (EdZ). Under the measurable condition, the former EDZ is defined as the rock zone where new macro fractures will occur (the minimum crack width is lager than 0.2 mm), and the later EdZ is the zone where deformation is obvious and micro fractures possibly measured by acoustic emission and sliding micrometer (the minimum crack width is less than 0.2 mm). Nowadays the digital borehole camera can recognize the smallest cracks with the minimum width of 0.2 mm [16, 17]. Therefore, it is possible for the technology to be adopted to observe the macro fractures and determine the EDZ.

3.2 Experimental schemes

There are two kinds of monitoring sections for the EDZ measurement, as shown in Figure 1. One is M1, used for obtaining deformation, cracks and elastic wave of rock mass by sliding micrometer, digital borehole camera and acoustic wave equipment. All the boreholes are parallel with a spacing of 1.5 m except for the two boreholes used for acoustic wave (1.0 m spacing). The other kind of section is M2 and is used for micro fractures of surrounding rock mass measured by acoustic emission apparatus. The layouts of boreholes are often designed to be rectangular and star shaped, as shown in Figure 3.

For experimental zones shown in Figure 1, JPTSA-2 has one M1 and one M2, but there are two M1 and one M2 in JPTSA-3. JPTY-21 has one M2 and one borehole of digital borehole camera (SZ1-1).

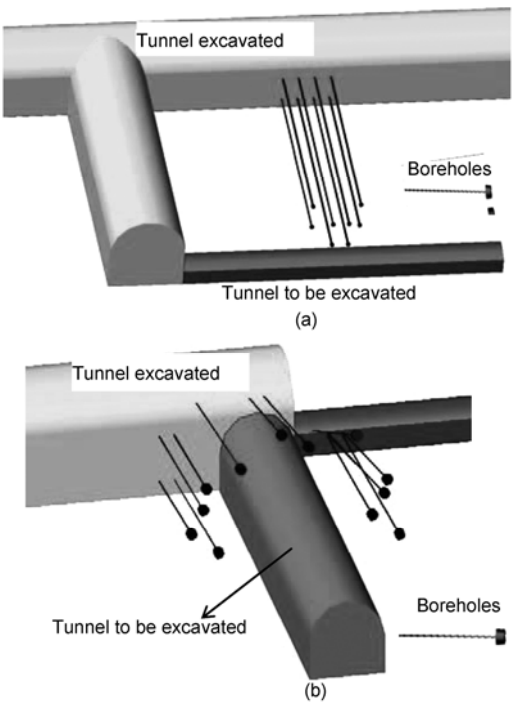

Figure 3 Boreholes configuration of acoustic emission in deeply buried tunnels of Jinping II hydropower station. (a) Rectangle configuration; (b) star configuration.

4 Results and discussions

4.1 Width of EDZ in JPTSA-2 experimental zone

For the JPTSA-2 experimental zone, the distance between the side wall of branch tunnel *C* and the testing boreholes orifice is 26.1 m. The experiment is to investigate the excavation damaged zone characteristics of branch tunnel *C*. Digital borehole camera in monitoring section M1 observes the macro-fracturing zone EDZ and the outer disturbed zone EdZ is determined by the deformation and elastic wave of tunnel surrounding rock mass.

According to the results of the digital borehole camera shown in Figure 3, the ultimate boundary of new cracks can be observed from the distance of 2.35 m (26.1−23.75=2.35 m) from the sidewall of branch tunnel *C*. Crack occurrence is N37ºW, ∠87º. For zone I shown in Figure 4, the width of the crack increases form 2 to 6 mm, while the maximum width of the crack in zone II is up to 5 mm. Thus, this position can be regarded as the ultimate boundary for the macro-fracturing zone.

In order to determine the outer disturbed zone, deformation and elastic wave of surrounding rock mass at monitoring section M1 are monitored during the whole excavation process and afterwards, the results are arranged and shown in Figures 5 and 6, respectively.

At the borehole depth of 17.3 m, it can be seen that elastic wave decreases significantly, where the deformation of rock mass increases with the tunnel excavation as well. The position is 8.8 m (26.1−17.3=8.8 m) from the sidewall of branch tunnel *C*. Therefore, this position is considered the ultimate boundary of the outer disturbed zone.

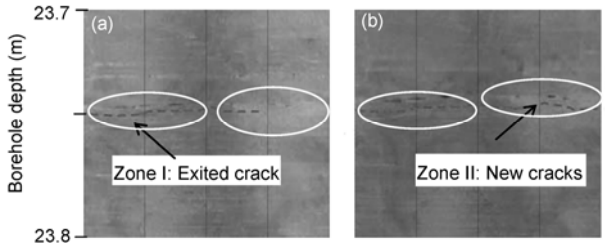

Figure 4 Fracture characteristics by digital borehole camera of monitoring section M1 in JPTSA-2 experimental zone. (a) Before excavation; (b) after excavation.

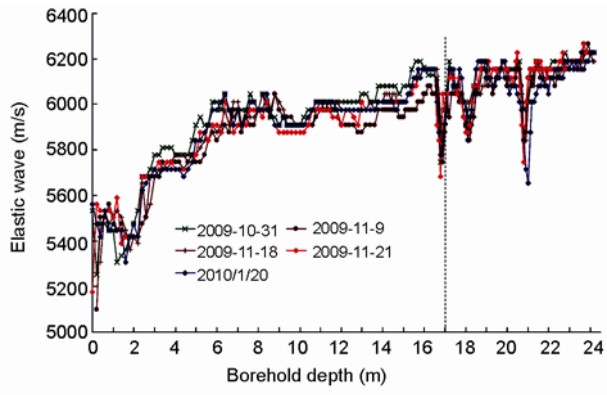

Figure 5 Results of elastic wave of monitoring section M1 in JPTSA-2 experimental zone.

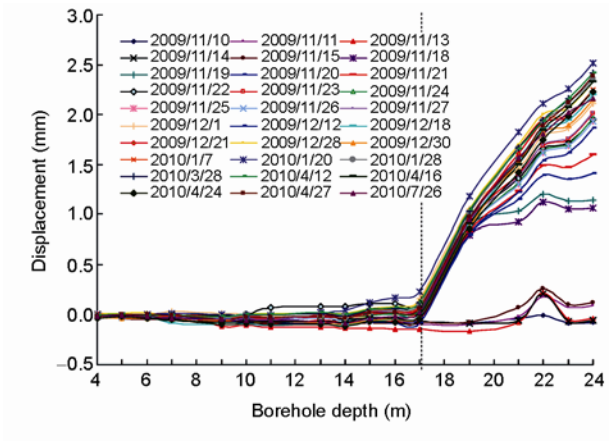

Figure 6 Displacement of monitoring section M1 over excavation time in JPTSA-2 experimental zone.

The final result of the EDZ width of branch tunnel *C* in JPTSA-2 zone is drawn in Figure 7, that is, the width of the macro-fracturing zone is 2.35 m, and the outer disturbed zone is up to 6.45 m (8.8−2.35= 6.45 m).

4.2 Width of EDZ in JPTSA-3 experimental zone

JPTSA-3 experimental zone has two branch tunnels of *B* and *F* with arch shape, each having a different geometric size. For the EDZ measurement, macro-fracturing zones are determined by digital borehole camera and the outer disturbed zones are obtained from deformation monitoring of surrounding rock mass.

For the branch tunnel *B*, the distance between the tunnel side wall and testing boreholes orifice is 24.0 m. The results from the digital borehole camera indicate that the ultimate boundary of new cracks is 5.2 m (24−18.8=5.2 m) from the tunnel sidewall as shown in Figure 8. The widths of new cracks 1, 2 and 3 are 1.5 mm, 10 mm and 15 mm, respectively.

On the other hand, the deformation of surrounding rock mass obtained by micro-sliding meter is shown in Figure 9,

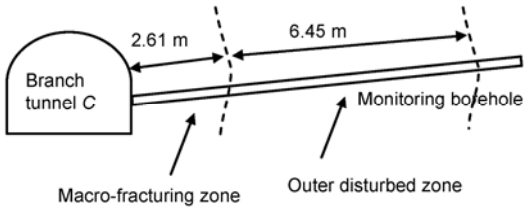

Figure 7 Sketch map of EDZ distribution of branch tunnel *C* in JPTSA-2 experimental zone.

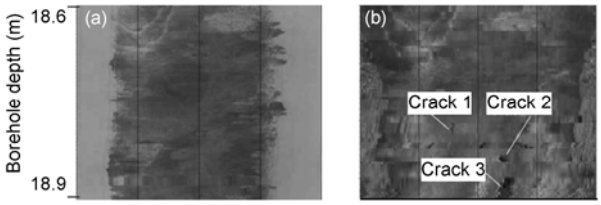

Figure 8 Fractures characteristic by digital borehole camera of monitoring section M1 of branch tunnel *B* in JPTSA-3 experimental zone. (a) Before excavation; (b) after excavation.

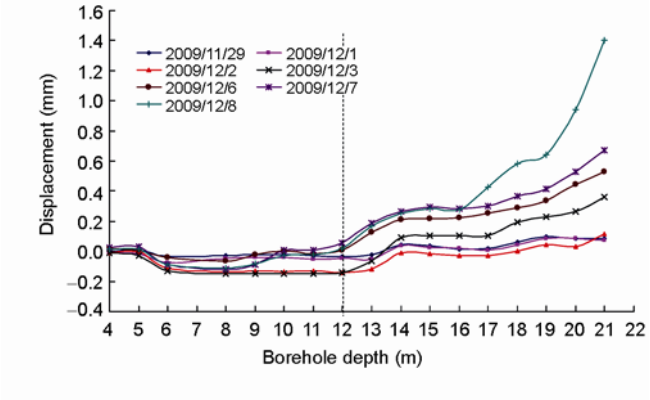

Figure 9 Deformation results of monitoring section M1 of branch tunnel *B* in JPTSA-3 experimental zone.

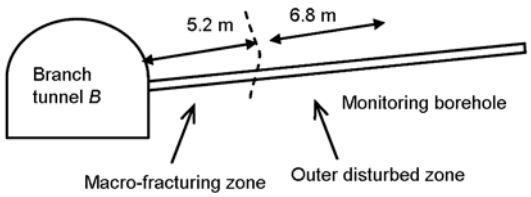

Figure 10 Sketch map of EDZ distribution of branch tunnel *B* in JPTSA-3 experimental zone.

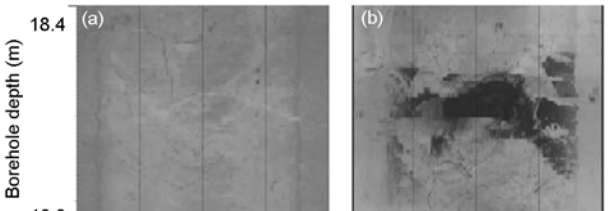

Figure 11 Fractures characteristic by digital borehole camera of monitoring section M1 of branch tunnel *F* in JPTSA-3 experimental zone. (a) Before excavation; (b) after excavation.

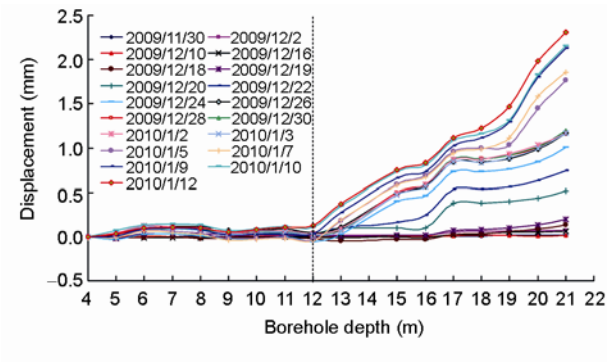

Figure 12 Deformation results of monitoring section M1 of branch tunnel *F* in JPTSA-3 experimental zone.

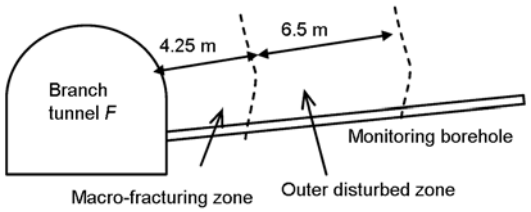

Figure 13 Sketch map of EDZ distribution of branch tunnel *F* in JPTSA-3 experimental zone.

which indicates that the obvious change of deformation is at the borehole depth of 12.0 m with the distance of 12.0 m (24.0−12.0=12.0 m) away from the tunnel sidewall, so the position is regarded as the ultimate boundary of the outer disturbed zone. By integrating the divisions of macro-fracturing zone, the final results of EDZ distribution can be expressed in Figure 10.

For the branch tunnel *F*, the distance between the tunnel sidewall and testing boreholes orifice is 22.75 m. The results from the digital borehole camera indicate that the ultimate boundary of new cracks formation is at the borehole depth 18.5 m. The position is 4.25 m away from the tunnel sidewall, as shown in Figure 11.

The displacement of surrounding rock mass is shown in Figure 12, and it can be seen that the obvious deformation occurs at the depth of 12.0 m with the distance 10.75 m away from the tunnel sidewall. Therefore, the widths of the macro-fracturing zone and the outer disturbed zone are 4.25 m and 6.5 m, respectively. The sketch map of EDZ distribution is shown in Figure 13.

4.3 Width of EDZ in JPTSA-21 experimental zone

In JPTSA-21 experimental zone, the objective is to investigate the EDZ of No.3 headrace tunnel excavated by TBM through branch tunnel 2-1. Borehole SZ1-1 uses digital borehole camera and monitoring section M2 uses acoustic emission.

From the analysis on a series of images obtained in borehole SZ1-1, the ultimate boundary of new crack formation is at the borehole depth of 19.5 m, i.e., 2.7 m away from the sidewall of No.3 headrace tunnel, as shown in Figure 14. Most of the crack occurrence is about N27°W, ∠53°, and the width of new cracks ranges from 1 to 3 mm.

According to the acoustic emission monitoring in Figure 15, most of the micro fractures and main damages in the

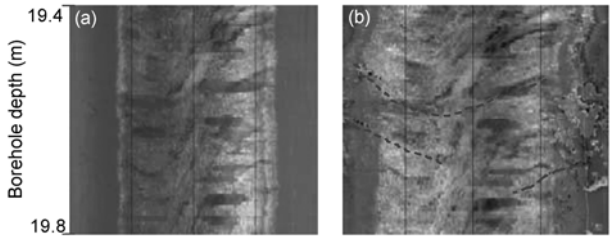

Figure 14 Fractures characteristic by digital borehole camera of SZ1-1 of No.3 headrace tunnel in JPTSA-21 experimental zone. (a) Before excavation; (b) after excavation.

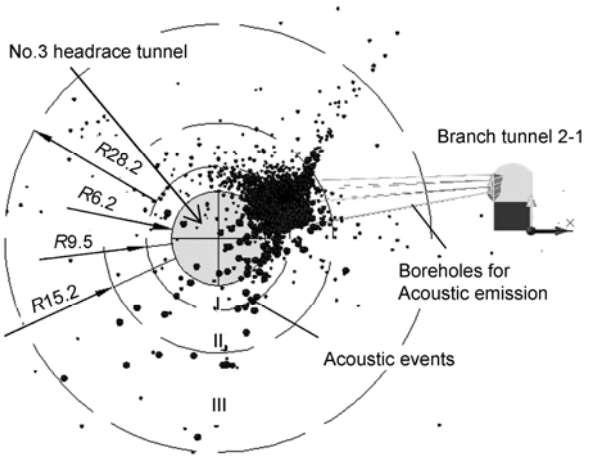

Figure 15 Acoustic emission around No.3 headrace tunnel in JPTSA-21 experimental zone.

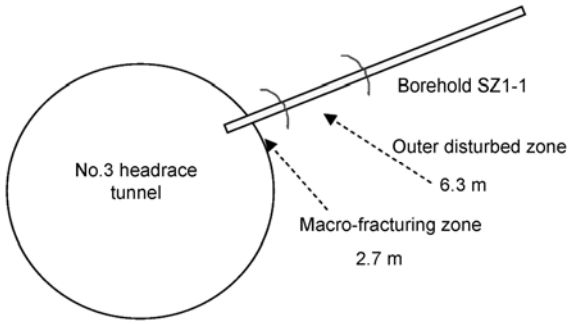

Figure 16 Sketch map of EDZ distribution of No.3 headrace tunnel in JPTSA-21 experimental zone.

surrounding rock mass concentrate at the range of 0 to 9.0 m away from sidewall of no.3 headrace tunnel. Based on the analysis above, the macro-fracturing zone is determined to be 2.7 m and the outer disturbed zone is 6.3 m (9.0–2.7=6.3 m). The distribution of EDZ is shown in Figure 16.

4.4 Influence factors and variation law of EDZ

According to the results described above, the widths of the EDZ in different conditions are arranged in Table 3.

In order to discuss the influence factors and variation law of EDZ, firstly, two parameters R_{ew} and R_{eh} are determined as

$$R_{ew} = ew / w,\ R_{eh} = ew / h, \tag{1}$$

where ew is the width of the macro-fracturing zone, and w and h are the width and height of the tunnel section, respectively.

Table 3 EDZ statistics on deep buried testing tunnels in Jinping II hydropower station

Tunnel No.	Width of excavation damaged zone (m)		Tunnel section (m)		Relationship with tunnel geometry		Excavation method
	EDZ (ew)	EdZ (dw)	Width (w)	Height (h)	R_{ew}	R_{eh}	
Branch tunnel *B*	5.2	6.8	5.0	5.0	1.1	1.1	D & B [a] (Full face)
Branch tunnel *C*	2.35	6.35	3.0	2.2	0.78	1.1	D & B (Full face)
Branch tunnel *F*	4.25	6.5	7.5	8.0	0.57	0.53	D & B (Two benches)
No.3 headrace tunnel	2.7	6.3	ϕ12.4		0.22		TBM (Full face)

a) Drilling and blasting.

From the statistical results in Table 3, it obviously seems that the widths of the EDZ are totally different for individual tunnels. The main factors influencing the EDZ include overburden depth, tunnel section and geometry, excavation method, stress field, lithology, joints, etc. However, compared to tunnel geometry, the widths of tunnels within the EDZ still have some variation described as follows:

(1) Under the same condition of lithology, overburden depth and excavation method, the width of the macro-fracturing zone is almost equal to the tunnel's geometric size. For example, R_{ew} and R_{eh} of branch tunnels *B* and *C* are in the range of 0.78–1.1.

(2) For those tunnels with the same lithology and overburden, but with different excavation methods, the width of the EDZ by two benches excavation is less than that by full face excavation. It can be seen in Table 3 that branch tunnels *B* and *C* were excavated by full face, but the tunnel *F* was excavated by partial face with an upper thickness of 5.0 m and lower thickness of 3.0 m. R_{ew} and R_{eh} of branch tunnel *F* are only 0.57 and 0.53, respectively.

(3) TBM tunnel has a smaller macro-fracturing zone than those tunnels excavated by the drilling and blasting method. For example, R_{ew} of no.3 headrace tunnel is only 0.22, which is almost one fifth of that in the drilling and blasting tunnels *B* and *C*.

4.5 Analysis on the characteristics of EDZ formation and evolution in deeply buried tunnels

Due to the excavating disturbances, the stress acting on the rock mass will redistribute and the rock mass adjacent to the excavated surface will entirely or partially yield, leading to

the EDZ formation. Fractures and deformation will occur because of the change of stress condition of EDZ rock mass. According to the in situ testing of the EDZ conducted during the whole construction process, the EDZ formation and its evolution show some typical characteristics, which are described as follows.

(1) EDZ formation occurs at the first stage of field geo-stress disturbance due to tunnel excavation which induces the fractures and deformation in rock mass ahead of working face. The influence range, however, should be controlled by a tunnel's geometric size, overburden depth and excavation methods. One example from No.3 headrace tunnel shows that TBM excavation will have direct impact on the rock mass ahead of working face. The scope of influence is at least up to 24.93 m (about two times of the tunnel diameter). One result from digital borehole SZ1-1 in experimental zone JPTSA-21 is shown in Figure 17. The width of original crack has some obvious changes, it reduced from 9.0 mm to 8.0 mm on the left part, but it increased from 4.5 mm to 8.1 mm on the right part. It seems that the rock mass has shear and tension deformation due to the TBM excavation disturbance.

(2) As the excavation continues, when the rock mass is under the condition of sudden unloading, the range of the EDZ will develop immediately. New cracks at the macro-fracturing zone of the EDZ have mixed characteristics of unloading, blasting and vibrating effects. The testing results indicate that the new cracks in this area, with widths ranging from 2.0 to 30.0 mm, almost do not have the same occurrence especially for drilling and blasting excavation method.

(3) After tunnel excavation, the stress redistribution process will continue in surrounding rock mass, but the damaging development will gradually converge. The time for convergence will be determined by the tunnel's geometric size, burial depth and excavation methods. At this stage, new crack formation and the exited fractures modification, development and closure are still observed in some cases.

There is a typical example of EDZ formation and evolution from branch tunnel C. A series of images of the borehole wall in monitoring section M1 obtained by digital borehole camera are analyzed, as shown in Figure 18.

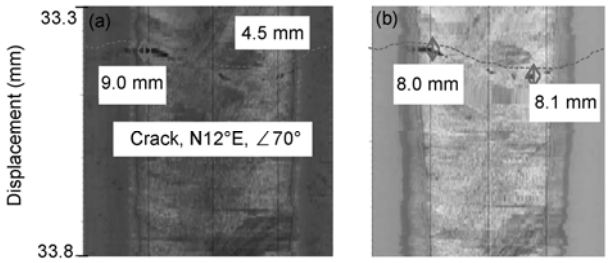

Figure 17 Characteristics of cracks ahead of TBM face in No.3 headrace tunnel in JPTSA-21 experimental zone interpreted by images of borehole wall, where *S* is the distance between borehole section and TBM face. (a) *S*=–46.85 m; (b) *S*=–24.93 m.

At the borehole depth of 23.75 m, before tunnel excavation began (October 20, 2009), the width of exited crack in zone I was 2 mm, and there was no crack in zone II, as shown in Figure 18(a). As the tunnel excavation continued, on October 22, 2009, the working face just passed the monitoring section where the borehole for the digital camera exited, new cracks formed in zone II and the old crack in zone I developed with the width increasing to 5 mm as shown in Figure 18(b). On November 27, 2009, the excavation of testing tunnel *C*, with a total length of 30 m, finished. As the working face passed the monitoring section, the distance between working face and borehole axis became 6.5 m and cracks developed continuously, as shown in Figure 18(c). On March 28, 2010, 120 days after the tunnel excavation ended, the old cracks closed but two new cracks with a width of 5mm formed nearby, as shown in Figure 18(d). Afterwards, on August 9, 2010, 261 days after the tunnel excavation ended, Figure 18(e) shows that the new cracks developed further and the crack in zone I increased to 9 mm, while the new cracks in zone II ran through, but the crack width reduced to 2 mm.

5 Conclusions

This paper presents in situ experiments on width and evolu-

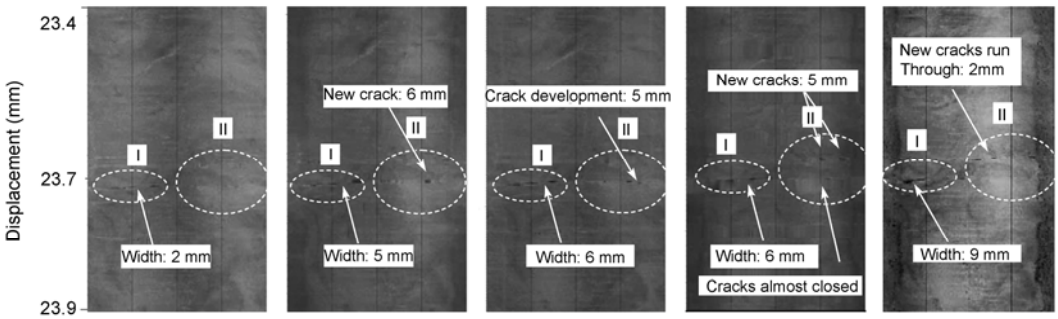

Figure 18 EDZ formation and evolution observed by digital borehole camera in branch tunnel C. (a) 2009/10/20; (b) 2009/11/22; (c) 2009/11/27; (d) 2010/03/28; (e) 2010/08/19.

tionary characteristics of EDZ in deeply buried test tunnels of the Jinping II hydropower station. A series of synthetic monitoring method were applied, some conclusions can be drawn as follows:

(1) The comprehensive testing methods of acoustic wave by two boreholes, digital borehole camera, sliding micrometer and acoustic emission provide some direct information for the EDZ measurement, such as velocity of sound waves, cracks, deformation and micro fractures of rock mass. The data collected from these measurements are important for the evaluation of mechanical characteristics of rock mass, rock burst and tunnel support design.

(2) Under the same condition of geological settings, geo-stress, burial depth and excavation methods, for drilling and blasting tunnels with full face excavation the EDZ are 0.78 to 1.1 times the tunnels' geometric sizes. On the other hand, under the same condition the EDZ excavated by two benches is less than that of full face. In addition, the surrounding rock mass of TBM tunnels receives obvious less damage than that of drilling and blasting tunnels, the EDZ is only 0.22 times of the tunnel's diameter.

(3) The formation of the EDZ occurs at the initial phase of field geo-stress disturbance due to tunnel excavation. After the sudden unload acting on surrounding rock mass by tunnel excavation, the range of the EDZ will develop immediately, with new cracks at the macro-fracturing zone having the mixed characteristics of unloading, blasting and vibrating effects.

(4) In the long-term run of deeply buried tunnels, the EDZ is continually changed. Some phenomena such as fractures modification, formation, development and closure can still be observed.

This work was supported by the National Basic Research Program of China ("973" Program) (Grant No. 2010CB732006) and the National Natural Science Foundation of China (Grant No. 40902091), the research was also supported by the CAS/SAFEA International Partnership Program for Creative Research Teams. The authors would also like to thank Ertan Hydropower Development Company, LTD, East China Investigation and Design Institution Under CHECC and China Railway Erju Co., Ltd..

1 Aston T R C, Gilby J L, Yue C M K. 2A comparison of rock mass disturbance in TBM and drill and blast drivages at the Donkin Mine, Nova Scotia. Int J Min Geol Eng, 1988, 6: 147–162
2 Pan P Z, Feng X T, Hudson J A. Study of failure and scale effects in rocks under uniaxial compression using 3D cellular automata. Int J Rock Mech Min Sci, 2009, 46(4): 647–685
3 Zhang C G, Wang J F, Zhao J H. Unified solutions for stresses and displacements around circular tunnels using the Unified Strength Theory. Sci China Tech Sci, 2010, 53(6): 1694–1699
4 Liu Y R, Chang Q, Yang Q. Fracture analysis of rock mass based on 3-D nonlinear Finite Element Method. Sci China Tech Sci, 2011, 54(3): 556–564
5 Zhang L Y, Mao X B, Lu A H. Experimental study on the mechanical properties of rocks at high temperature. Sci China Tech Sci, 2009, 53(3): 641–646
6 Kwon S, Lee C S, Cho S J, et al. An investigation of the excavation damaged zone at the KAERI underground research tunnel. Tunn Undergr Space Tech, 2009, 24(1): 1–13
7 Martino J B, Chandler N A. Excavation-induced damage studies at the underground research laboratory. Int J Rock Mech Min Sci, 2004, 41(8): 1413–1426
8 Read R S. 20 years of excavation response studies at AECL's underground research laboratory. Int J Rock Mech Min Sci, 2004, 41(8): 1251–1275
9 Cai M, Kaiser P K, Tasaka Y, et al. Generalized crack initiation and crack damage stress thresholds of brittle rock masses near underground excavations. Int J Rock Mech Min Sci, 2004, 41(5): 833–847
10 Egger P. Study of excavation induced rock damage at the grimsel underground rock laboratory. Nucl Eng Ng Des, 1989, 116: 11–19
11 Sato T, Kikuchi T, Sugihara K. *In-situ* experiments on an excavation disturbed zone induced by mechanical excavation in Neogene sedimentary rock at Tono mine, central Japan. Eng Geology, 2000, 56: 97–108
12 Yan P, Lu W B, Shan Y G. Detecting and study of blasting excavation-induced damage of deep tunnel and its characters (in Chinese). Chin J Rock Mech Eng, 2009, 28(8): 1552–1561
13 Stephen D, Falls l, Young R P. Acoustic emission and ultrasonic-velocity methods used to characterize the excavation disturbance associated with deep tunnels in hard rock. Tectonophysics, 1998, 289: 1–15
14 Kelsall P C, Case J B, Chabannes C R. Evaluation of excavation-induced changes in rock permeability. Int J Rock Mech Min Sci, 1984, 21(3): 123–135
15 Wu S Y, Shen M B, Wang J. Jinping hydropower project: main technical issues on engineering geology and rock mechanics. Bull Eng Geol Environ, 2010, 69: 325–332
16 Williamsa J H. Carole D. Johnson, Acoustic and optical borehole-wall imaging for fractured-rock aquifer studies. J Appl Geophys, 2004, 55: 151–159
17 Wang C Y, Law T K, Ge X R. Borehole camera technology and its application in the three gorges project, Proceedings of the 55th Canadian Geotechnical and 3rd Joint IAH-CNC and CGS groundwater specialty conferences, Niagara Falls, Ontario, 2002. 601–618